GSA Data Repository 2016332
Sulfur-oxidizing bacteria prior to the Great Oxidation Event from the 2.52-Ga Gamohaan Formation of South Africa

Andrew D. Czaja[1*], Nicolas J. Beukes[2], and Jeffrey T. Osterhout[1]

[1]Department of Geology, University of Cincinnati, PO Box 210013, Cincinnati, OH 45221-0013, USA
[2]Paleoproterozoic Mineralization Research Group, Department of Geology, University of Johannesburg, P.O. Box 524, Auckland Park, South Africa

SUPPLEMENTARY TEXT, FIGURES AND DESCRIPTIONS OF ASSOCIATED 3-D CLSM ANIMATIONS

GEOLOGIC CONTEXT

A black chert was collected from two localities within the Gamohaan Formation, Kaapvaal Craton, South Africa (see Figure 1 in the main text for map and stratigraphic column). One locality was 12.5 km NW of the town of Kuruman (27º 23' 0" S, 23º 20' 46" E) and the other was 8.5 km NNE of the town of Danielskuil (28º 06' 10" S, 23º 34' 12" E) in the Northern Cape Province (Fig. DR1-A and -B). The chert occurred as a thin layer (~10 cm, Fig. DR1-C and -D) that outcropped continuously over at least tens of meters at the Kuruman location (although the full extent was not measured), but also showed continuity over the ~80 km between the two localities. The chert is situated within a carbonate unit with sets of contorted fossil microbial mat structures interpreted as being deposited in deep water (Fig. DR1-D, Sumner, 1997). In addition, the finely layered nature (Fig. DR1-E and F) and extent of the unit provide evidence for deep-water deposition. Evidence for the activity of sulfur metabolism and that the fossils discovered here were sulfur oxidizers comes from the presence of pyrite-rich layers and nodules (now oxidized to Fe-oxides) present adjacent to the chert layer (Fig. DR1-D). Finely disseminated pyrite also occurs occasionally within the chert layers. It was from these layers that Kaufman et al. (2007) and Kamber and Whitehouse (2007) measured multiple sulfur isotopes of pyrite (see the Discussion section in the main text for more details).

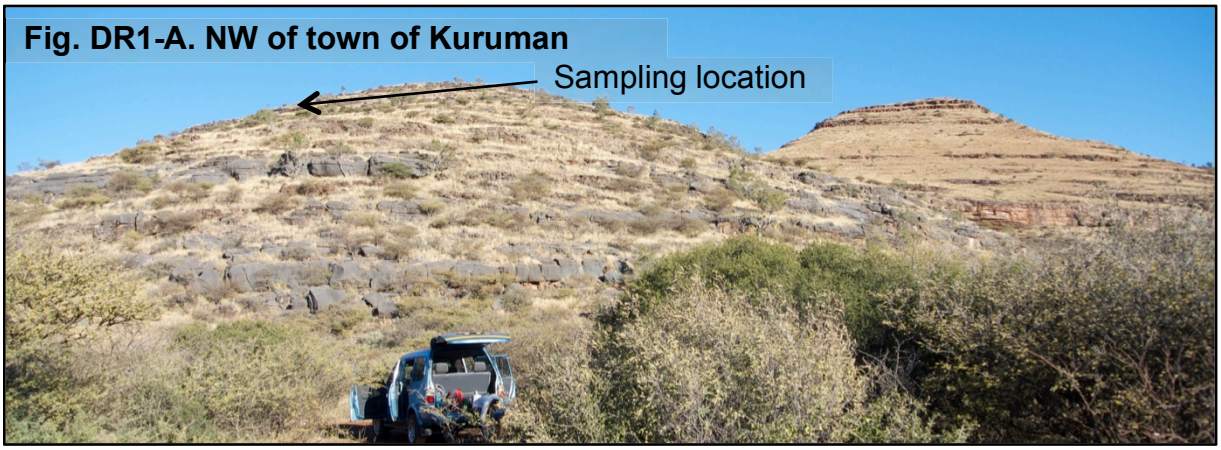
Fig. DR1-A. NW of town of Kuruman
Sampling location

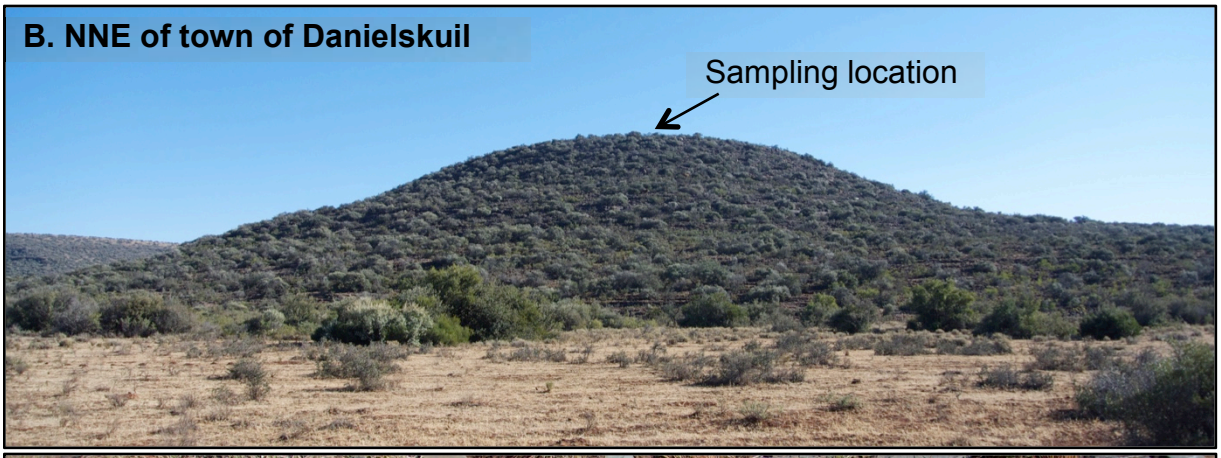
B. NNE of town of Danielskuil
Sampling location


C. Outcrop near Kuruman
Fossiliferous chert

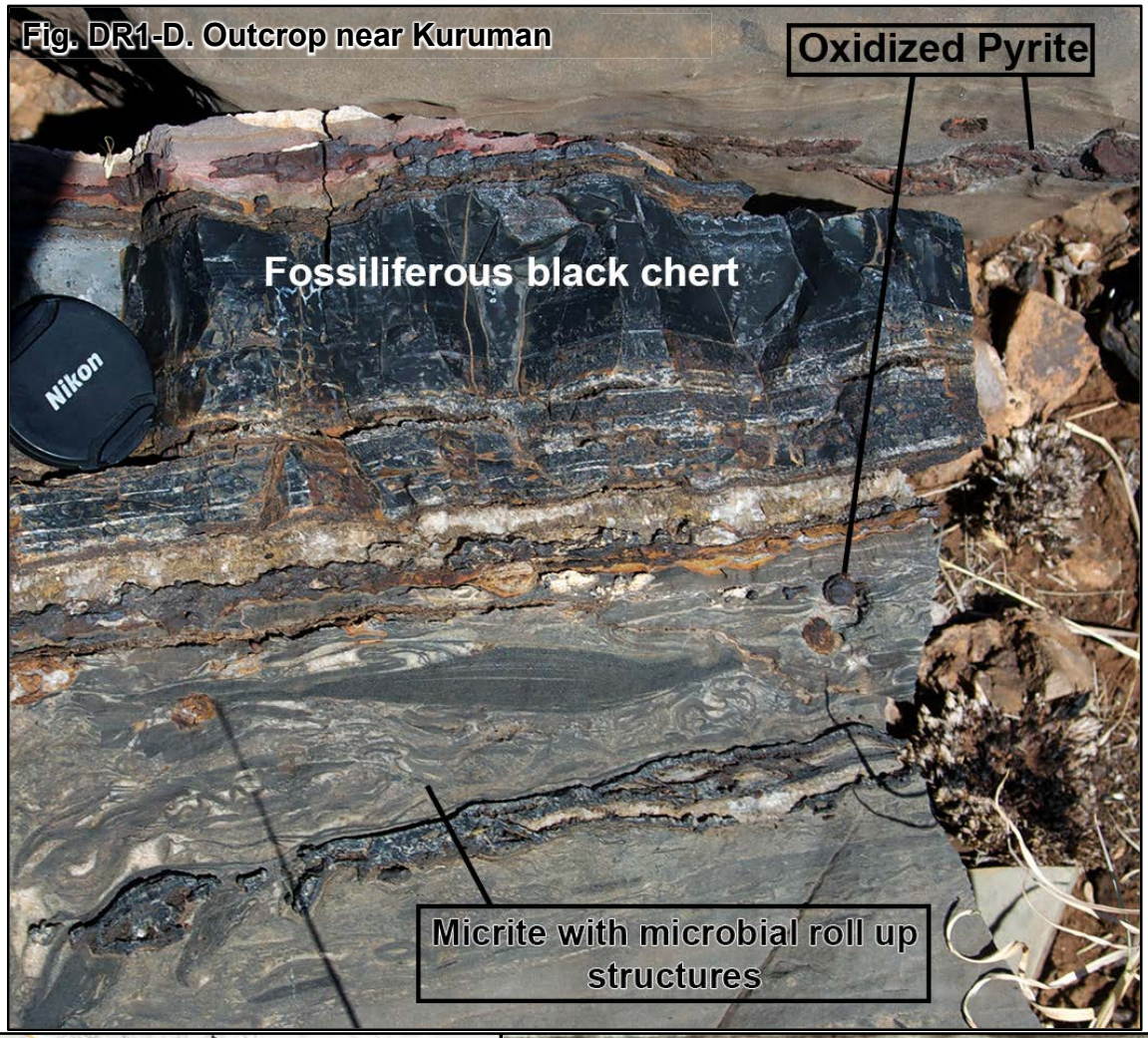
Fig. DR1-D. Outcrop near Kuruman
Oxidized Pyrite
Fossiliferous black chert
Nikon
Micrite with microbial roll up structures

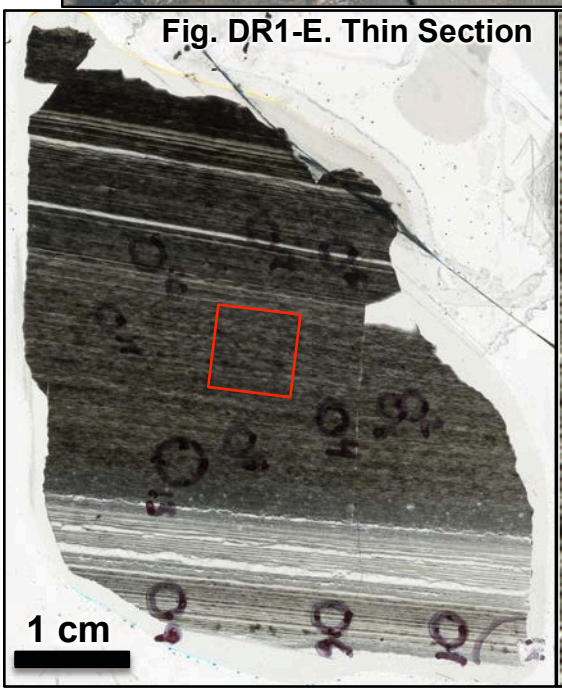
Fig. DR1-E. Thin Section
1 cm

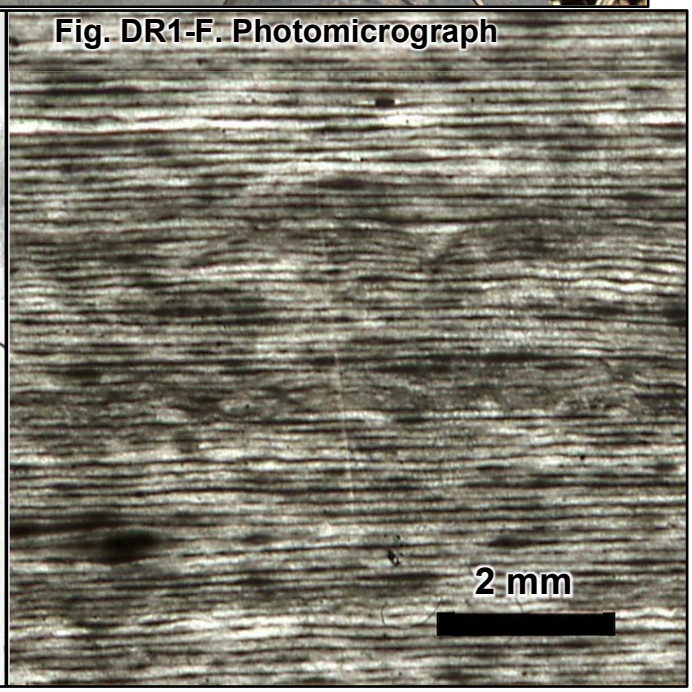
Fig. DR1-F. Photomicrograph
2 mm

SUPPLEMENTARY FOSSIL IMAGES

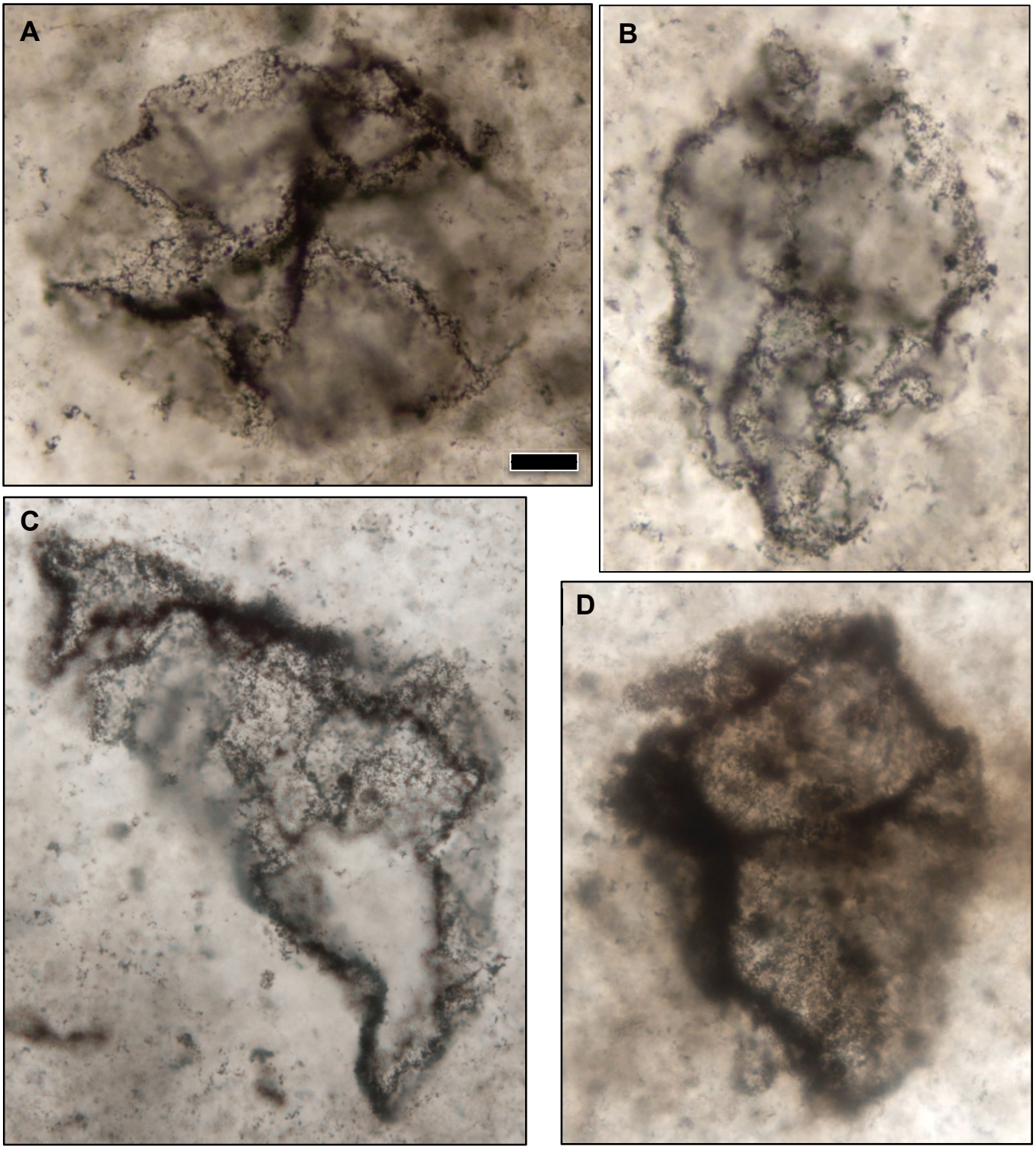

Figure DR2. Photomicrographs of selected large coccoidal fossils from the Gamohaan Formation imaged in thin sections cut parallel to the bedding plane. Fossils in panels A and B are the same as those in Fig. 2A and B in the main text. Fossils in panels A–EE imaged using a 20X or 40X objective. Scale bar in A is 25 μm and applies to all panels. All fossils are housed at the University of Cincinnati. See Table DR1 for thin section and stage coordinate information for each figured specimen.

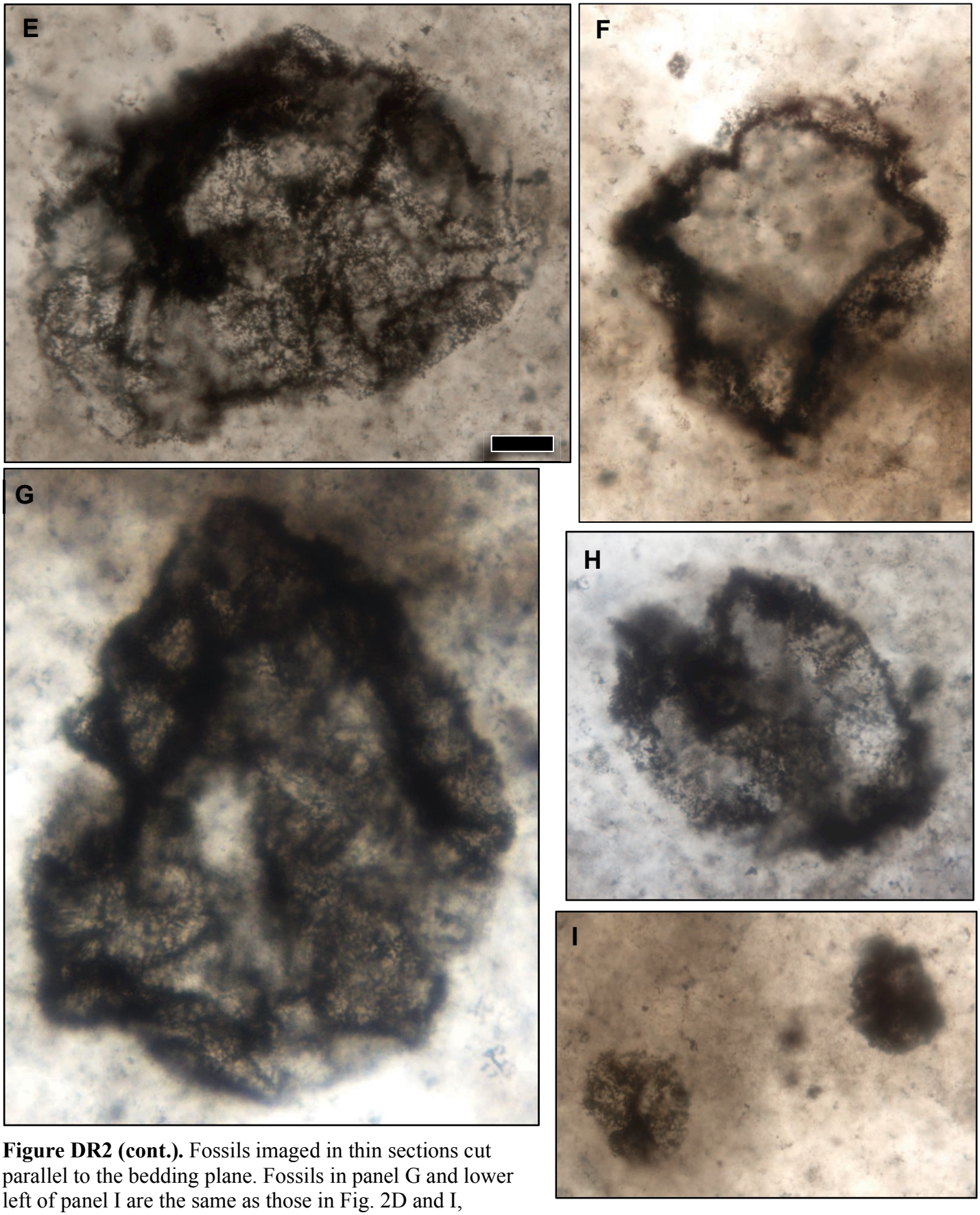

Figure DR2 (cont.). Fossils imaged in thin sections cut parallel to the bedding plane. Fossils in panel G and lower left of panel I are the same as those in Fig. 2D and I, respectively, in the main text. Scale bar in E is 25 μm and applies to all panels.

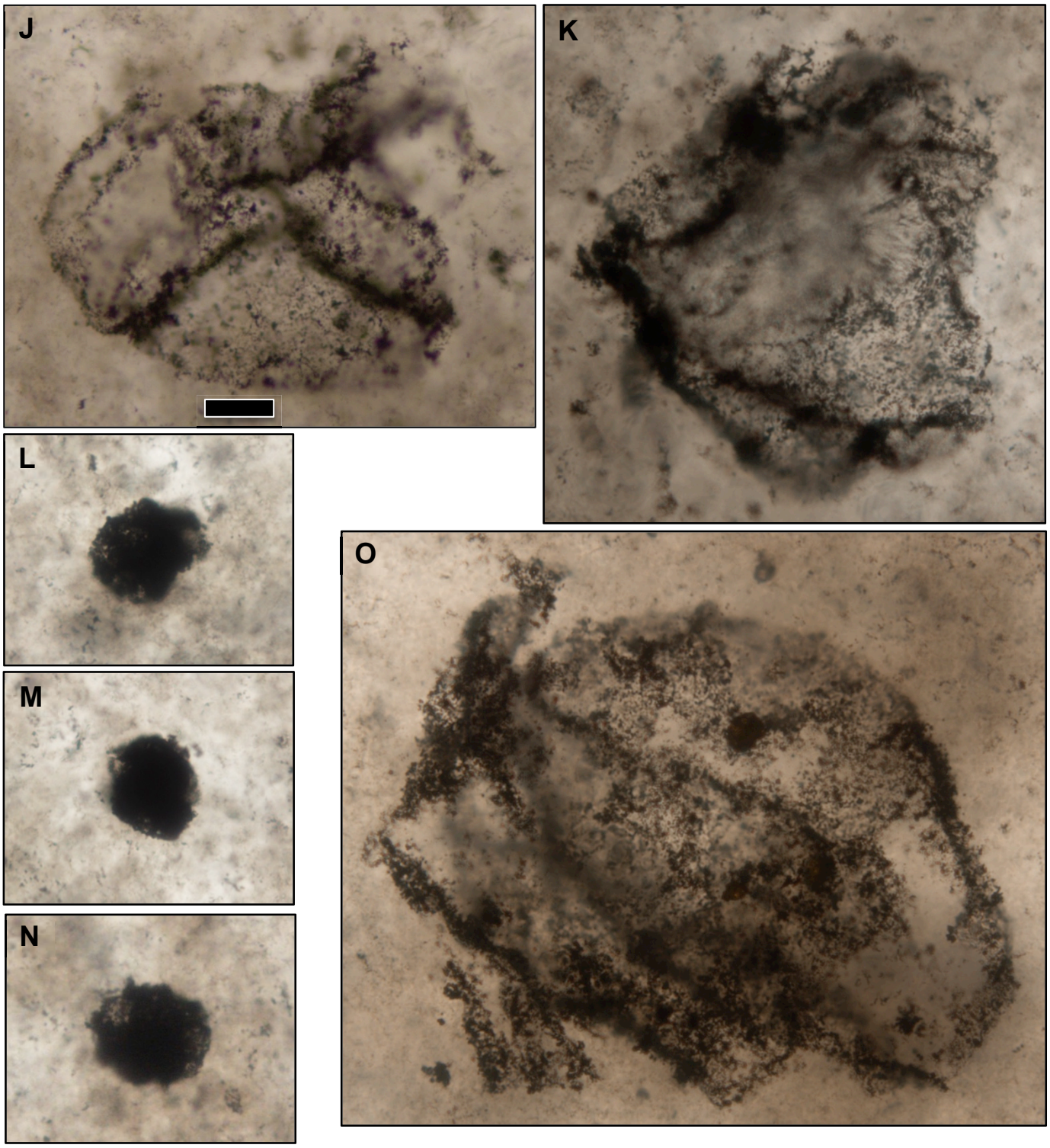

Figure DR2 (cont.). Fossils imaged in thin sections cut parallel to the bedding plane. Fossil in panel J is the same as that in Fig. 2E in the main text. Scale bar in J is 25 μm and applies to all panels.

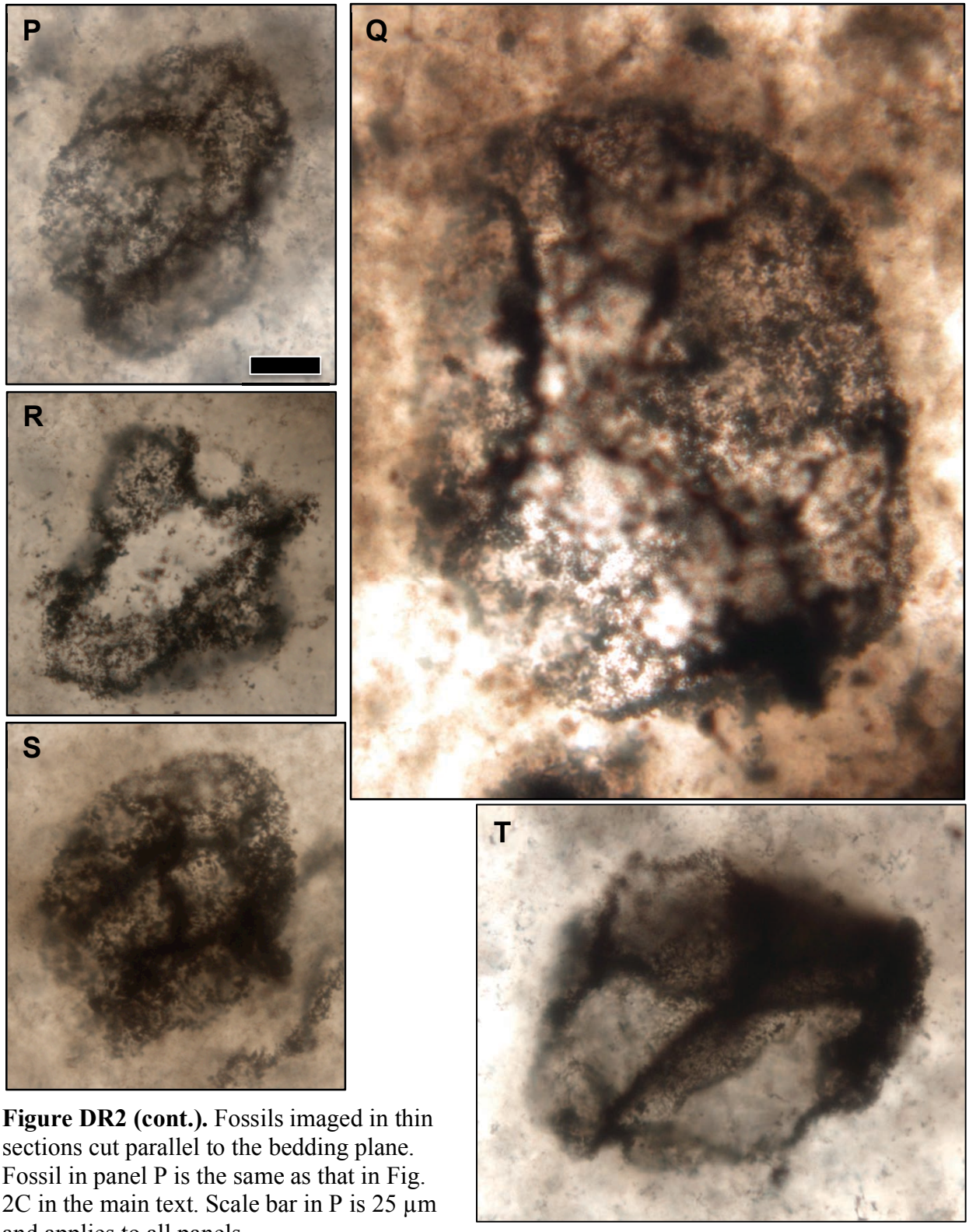

Figure DR2 (cont.). Fossils imaged in thin sections cut parallel to the bedding plane. Fossil in panel P is the same as that in Fig. 2C in the main text. Scale bar in P is 25 μm and applies to all panels.

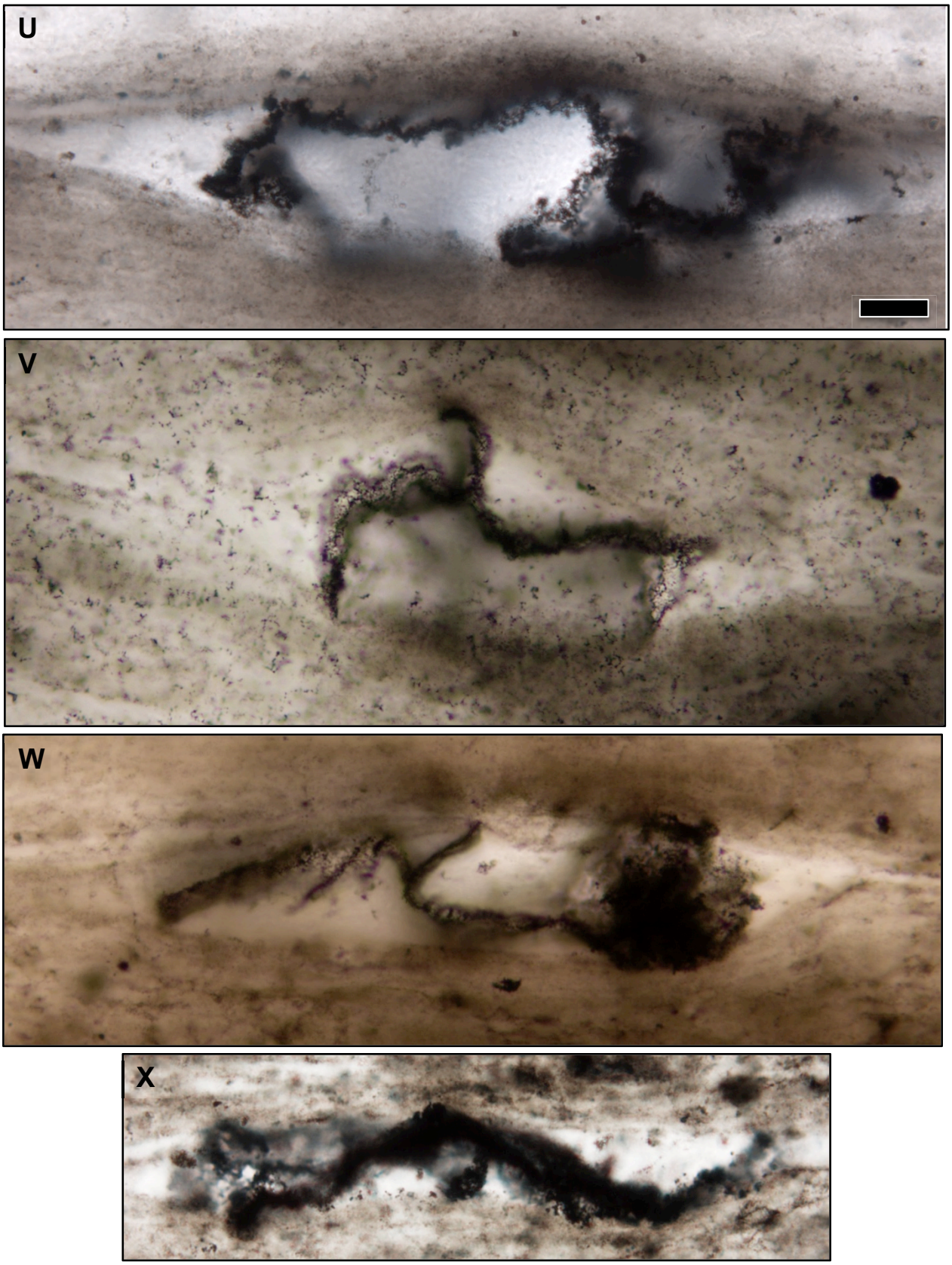

Figure DR2 (cont.). Fossils imaged in thin sections cut perpendicular to the bedding plane. Fossil in panel V is the same as that in Fig. 2N, respectively, in the main text. Scale bar in U is 25 μm and applies to all panels.

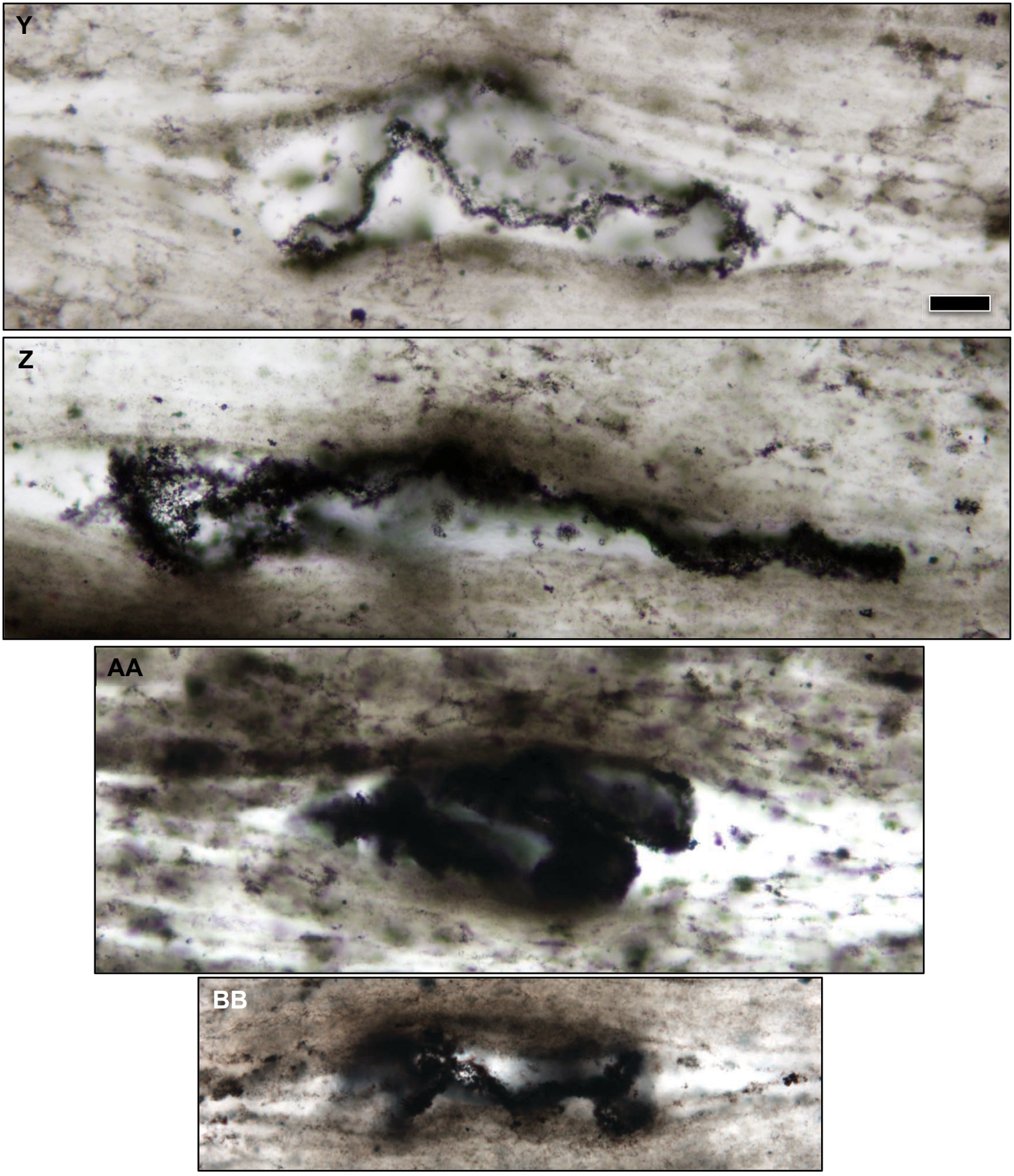

Figure DR2 (cont.). More fossils imaged in thin sections cut perpendicular to the bedding plane. Scale bar in Y is 25 μm and applies to all panels.

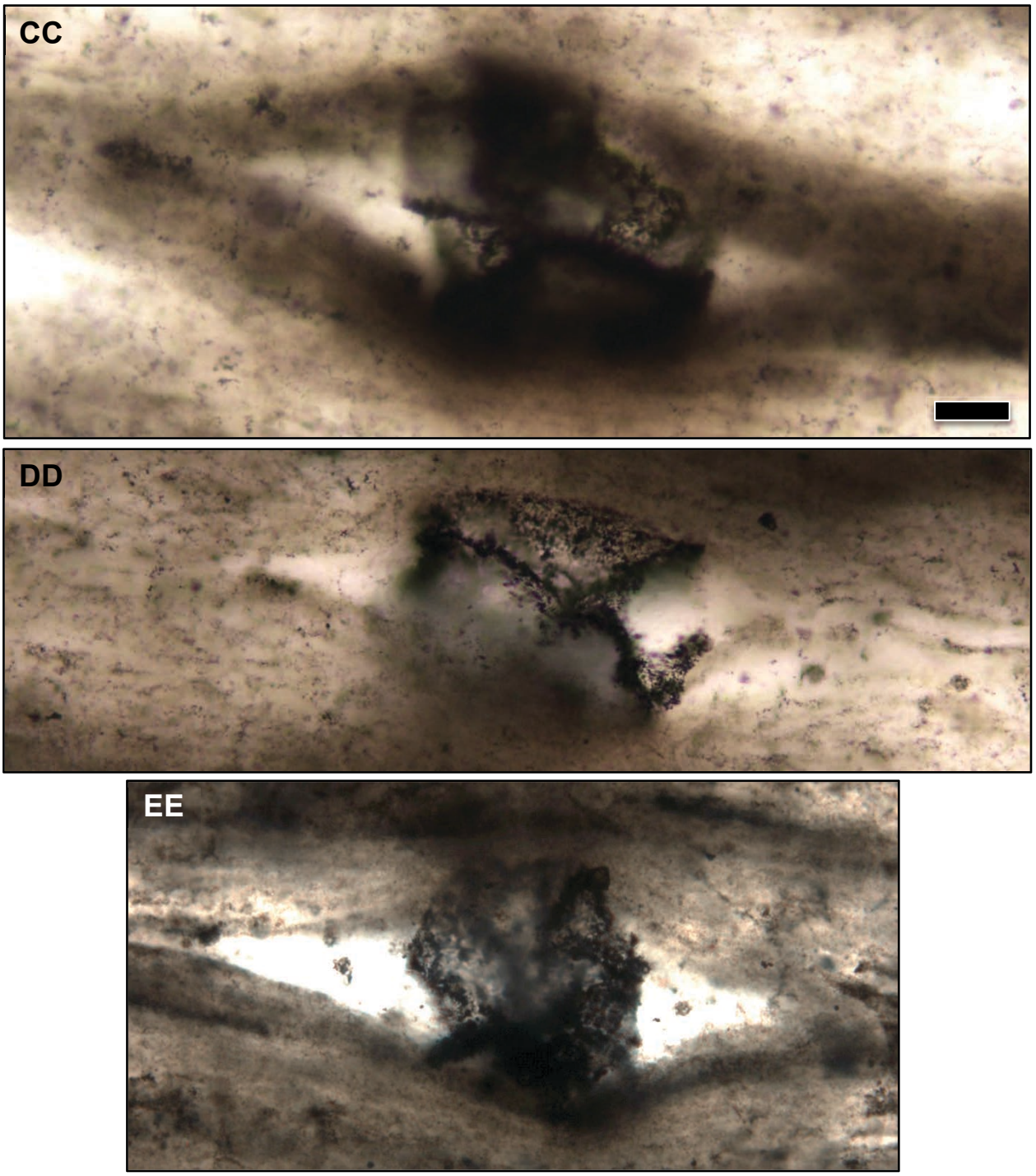

Figure DR2 (cont.). Fossils imaged in thin sections cut perpendicular to the bedding plane. Scale bar in CC is 25 μm and applies to all panels.

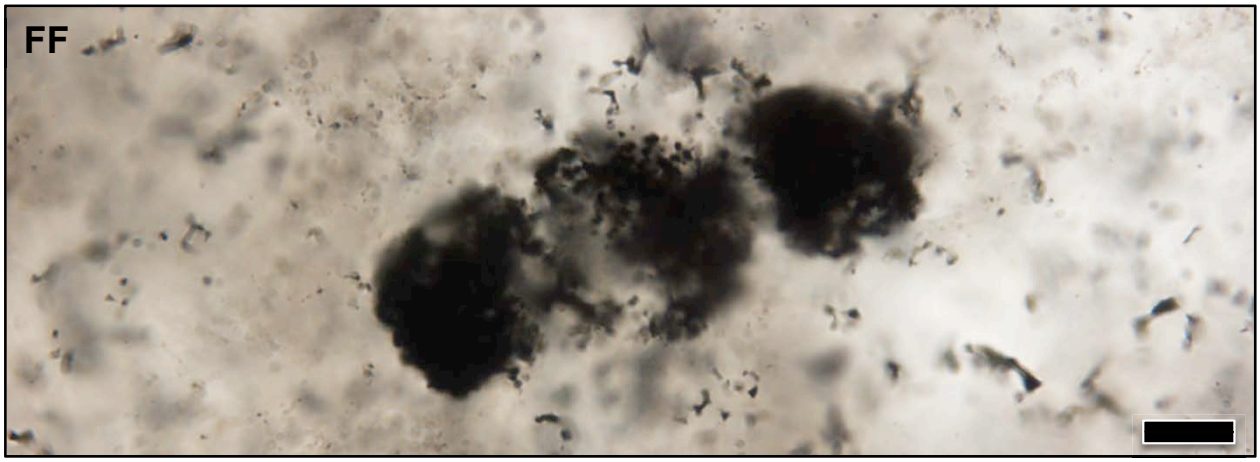

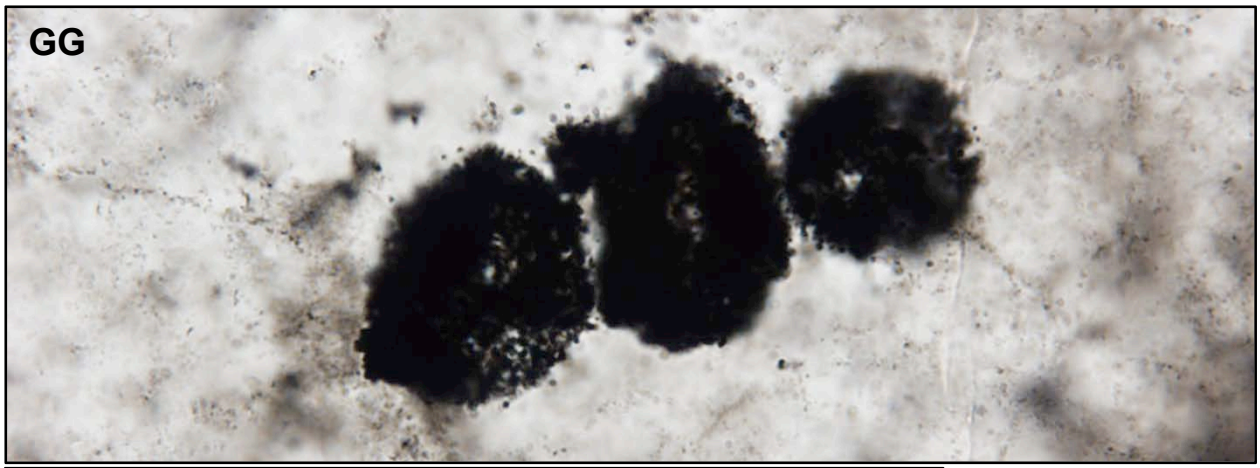

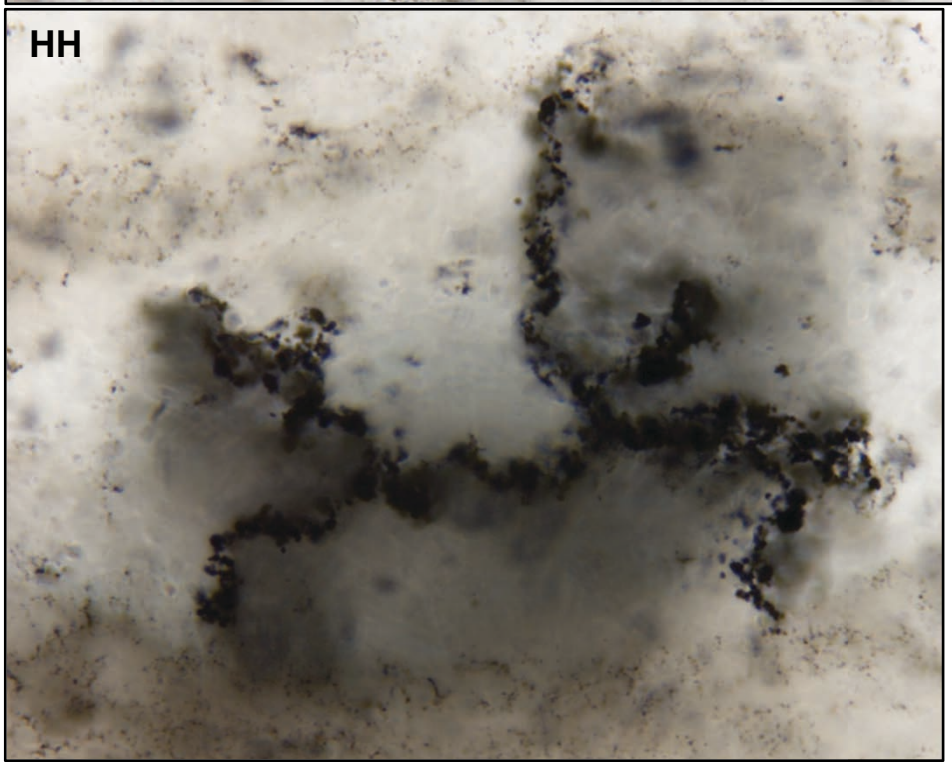

Figure DR (cont.). Photomicrographs of selected fossils in thin sections cut parallel to the bedding plane (FF and GG), and cut perpendicular to the bedding plane (HH). Fossils in panels FF and GG are the same as those in Fig. 2H and G, respectively, in the main text. Images taken with a 100X oil immersion objective. Scale bar in FF is 10 μm and applies to all panels.

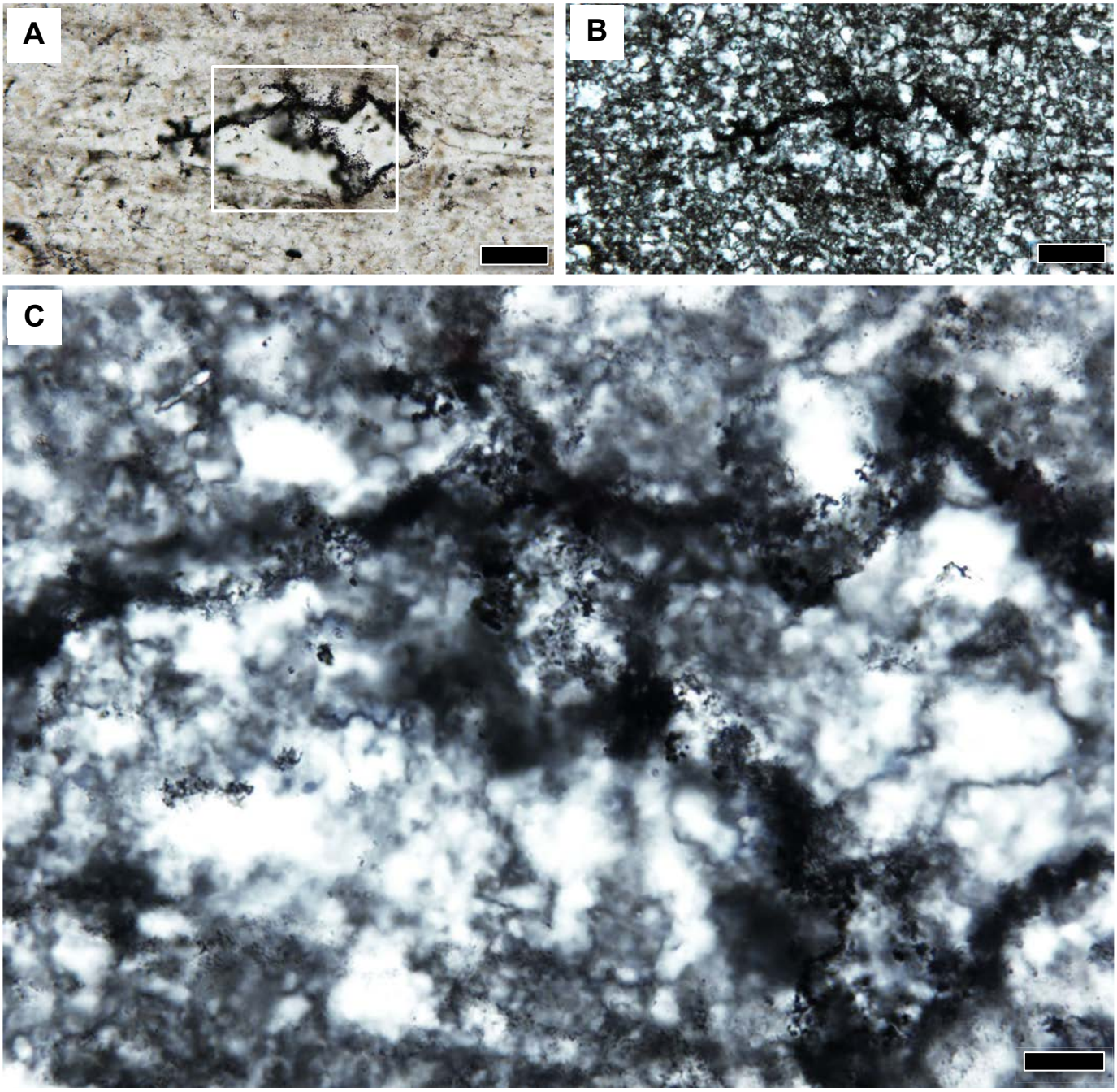

Figure DR3. Photomicrographs of selected fossils in thin sections cut perpendicular to bedding to illustrate the similarity of the quartz immediately surrounding the compressed fossil coccoid to that in the outlying chert matrix. A) Fossil imaged in transmitted white light showing typical compacted fossil form. B) Same fossil and field of view as panel A, but imaged in plane polarized light. C) Magnified view of the fossil and chert in panel B. There is no evidence of fan or rosette-like crystal forms that would indicate the object was formed by crystal growth. The white box in panel A indicates the region imaged in panel C. Fossil in panels A and B is the same as that in Figure 2L and M of the main text, respectively, and the images were taken with a 20X objective. Image in panel C was taken with a 100X oil immersion objective. Scale bars in A and B are 50 μm and that in panel C is 10 μm.

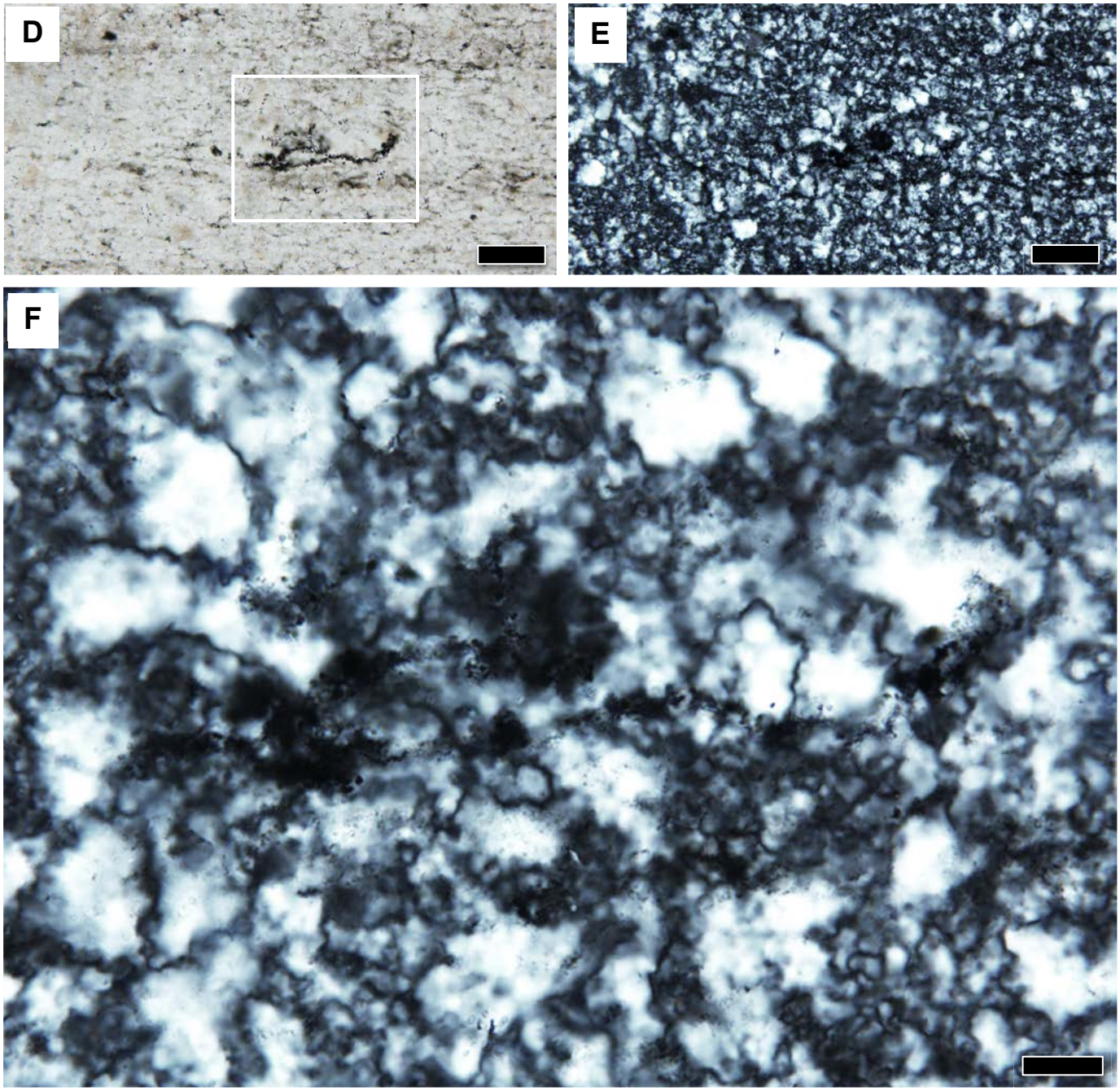

Figure DR3 (cont.). Photomicrographs of selected fossils in thin sections cut perpendicular to bedding to illustrate the similarity of the quartz immediately surrounding the compressed fossil coccoid to that in the outlying chert matrix. D) Fossil imaged in transmitted white light showing typical compacted fossil form. E) Same fossil and field of view as panel D, but imaged in plane polarized light. F) Magnified view of the fossil and chert in panel E. There is no evidence of fan or rosette-like crystal forms that would indicate the object was formed by crystal growth. The white box in panel D indicates the region imaged in panel F. Images in panels D and E were taken with a 20X objective. Image in panel F was taken with a 100X oil immersion objective. Scale bars in D and E are 50 μm and that in panel F is 10 μm.

Specimen locations

All specimens are housed in the PASTBIO Lab run by Andrew Czaja at the University of Cincinnati. Table DR1 lists the thin section ID and stage coordinates for each imaged specimen. All samples were located using an Olympus BX53 upright research microscope in the PASTBIO Lab.

Table DR1. Locations of all imaged fossil specimens

Specimen image	Locality	Thin section	Specimen number	Stage coordinates
Fig. 2A, DR2-A	Kuruman	GCB-13-1-2D(b)	13	132.6 x 21.8
2B, DR2-B	Kuruman	GCB-13-1-2D(b)	14	127.7 x 19.8
2C, DR2-P	Kuruman	GCB-13-1-2E(b)	06	123.5 x 32.1
2D, DR2-G	Kuruman	GCB-13-1-2E(b)	07	120.5 x 32.9
2E, DR2-J	Kuruman	GCB-13-1-2D(b)	12	128.4 x 22.9
2F	Kuruman	GCB-13-1-2E(b)	09	139.5 x 30.6
2G, DR2-GG	Danielskuil	GCB4-14-1-6D(b)	02	143.2 x 19.4
2H, DR2-FF	Kuruman	GCB-13-1-2E(b)	17	121.6 x 32.3
2I, DR2-I	Kuruman	GCB-13-1-2D(b)	08	152.9 x 27.5
2L,M, DR3-A–C	Kuruman	GCB-13-3-2A	09	142.2 x 9.2
2N,O, DR2-V	Kuruman	GCB-13-1-2A	10	146.8 x 36.8
Fig. DR2-C	Kuruman	GCB-13-1-2E(b)	11	132.4 x 28.3
DR2-D	Kuruman	GCB-13-1-2E(b)	13	142.3 x 21.9
DR2-E	Kuruman	GCB-13-1-2D(b)	11	118.5 x 23.1
DR2-F	Kuruman	GCB-13-1-2E(b)	14	130.6 x 18.7
DR2-H	Kuruman	GCB-13-1-2D(b)	15	156.5 x 26.7
DR2-K	Kuruman	GCB-13-1-2D(b)	04	129.9 x 29.3
DR2-L	Kuruman	GCB-13-1-2D(b)	05A	154.0 x 29.6
DR2-M	Kuruman	GCB-13-1-2D(b)	05B	154.0 x 29.6
DR2-N	Kuruman	GCB-13-1-2D(b)	05C	154.0 x 29.6
DR2-O	Kuruman	GCB-13-1-2D(b)	06	138.4 x 26.2
DR2-Q	Danielskuil	GCB4-14-1-6C(b)	11	143.4 x 24.3
DR2-R	Kuruman	GCB-13-1-2D(b)	10	119.9 x 25.4
DR2-S	Kuruman	GCB-13-1-2D(b)	09	130.6 x 24.6
DR2-T	Kuruman	GCB-13-1-2E(b)	12	135.9 x 23.6
DR2-U	Danielskuil	GCB4-14-1-1A	01	137.6 x 35.3
DR2-W	Danielskuil	GCB4-14-1-5A	02	130.4 x 31.4
DR2-X	Kuruman	GCB-13-3-2A	02	145.3 x 33.6
DR2-Y	Kuruman	GCB-13-2-1B	01A	121.9 x 13.6
DR2-Z	Kuruman	GCB-13-3-1A	08	131.9 x 34.1
DR2-AA	Kuruman	GCB-13-3-1A	17	132.5 x 23.3
DR2-BB	Kuruman	GCB-13-3-2A	05	139.2 x 35.7
DR2-CC	Kuruman	GCB-13-1-2A	07	148.7 x 25.7
DR2-DD	Kuruman	GCB-13-1-2A	03	133.2 x 13.5
DR2-EE	Kuruman	GCB-13-3-1A	04	135.2 x 37.3
DR2-HH	Kuruman	GCB-13-3-1A	06	117.0 x 34.1
Fig. DR3-D–F	Kuruman	GCB-13-3-2A	10	142.2 x 7.7

Fossil aspect ratios

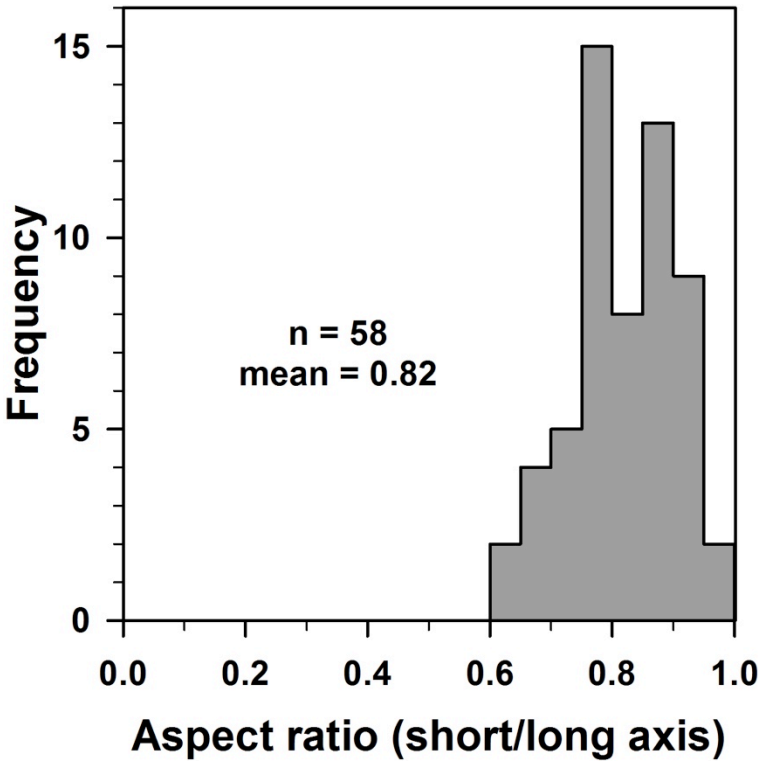

Figure DR4. Aspect ratio of fossils reported here, defined as the ratio of the short to long axes of the well-preserved fossils imaged in bedding plane thin sections. Only fossils imaged in thin sections cut parallel to the bedding plane are included in these compilations.

Confocal microscopy and image processing

Confocal laser scanning microscopic images were collected with an Olympus FV1200 microscope (Olympus, Inc., Shinjuku, Japan) using a 559 nm laser and a 60X oil immersion lens and no filter. The fossils did not produce sufficient fluorescence with excitation by 458, 488, 514, 559, or 633 nm lasers to produce useful images, unlike some less thermally altered fossils (e.g., Schopf et al., 2006; Schopf and Kudryavtsev, 2009; Schopf et al., 2016). Thus, reflected light images were produced. Two-dimensional images were collected with a confocal aperture of 65 µm. The effective maximum depth to which fossils could be imaged is 70 µm, due to attenuation of the signal caused by scattering of the laser light. Each original 2D image contained significant "noise" in the form of scattered light from kerogen or other objects in the surrounding matrix. Because this "noise" was caused by the same phenomenon as what produced the "signal", it could not be tuned out. The result was a 3D image that was greatly obscured. Transmitted light images were collected at the same focal depths and fields of view as the fluorescence images for each image slice. These were compared to the CLSM images and the "noise" was manually erased from each slice using ImageJ software (v. 1.50). Care was taken to

be conservative and leave in all parts of the fossil, with the result that there are occasional artifacts in some of the animations.

Three-dimensional image animations are attached as separate movie files. Images were collected with different x-y resolutions and z-spacings depending on the size of the fossil. Fossil animation **A**, which is also illustrated in Figure 2A and Figure DR2-A, was created from 138 x-y CLSM images of 756 x 643 pixels each (x-y pixel spacing of 0.265 μm and z-spacing of 0.4 μm). Animation **B**, also illustrated in Figure 2G and Figure DR2-GG, was created from 65 x-y CLSM images of 757 x 510 pixels each (x-y pixel spacing of 0.106 μm and a z-spacing of 0.31 μm). Animation **C**, also illustrated in Figure 2N and Figure DR2-V, was created from 97 x-y CLSM images of 446 x 640 pixels each (x-y pixel spacing of 0.254 μm and a z-spacing of 0.75 μm). The 2-D images were exported as TIF files and imported into the software program Paraview v. 5.0.1 (Kitware Inc., Clifton Park, NY), with which they were rendered into 3D images and animated.

Raman Index of Preservation

Fossil coccoids and background kerogen in the matrix were analyzed by Raman spectroscopy as described in the main text. The Raman spectra were collected by use of an Olympus BX41 microscope attached to the Horiba T64000 system (Horiba, Inc., Edison, NJ) with a 50X long working distance objective (NA = 0.50). Data were collected and processed using the software LabSpec (v.5; Horiba, Inc., Edison, NJ). To compare to previously published Raman spectra, the Raman spectra measured in this study were corrected with the system's response function, which was measured with a calibrated halogen light source. The relative degree of thermal alteration of the fossils was defined using the Raman Index of Preservation (RIP; Schopf et al., 2005). Backgrounds were minimal and were corrected by subtracting a simple linear baseline. Contributions from the minor quartz peak at ~1160 cm^{-1} were removed and spectral areas were integrated between 1100 and 1300 cm^{-1} (α value) and between 1300 and 1370 cm^{-1} (γ value). The RIP value was originally defined as the ratio of these two values (α/γ) normalized to a set of fossils of varying degrees of thermal alteration to make the fossils range in RIP from 1 to 9, with 9 being less thermally altered and 1 being more thermally altered (Schopf et al., 2005). To put the Gamohaan fossils on this scale a regression was fit to the RIP and integrals for the standard fossil data and the equation RIP = 7.6866*(α/γ). Table DR2 shows the

average RIP values measured for fossils and background kerogen showing that they are all consistent and thus experienced the same degree of alteration.

Table DR2. Average Raman Index of Preservation (RIP) values measured for fossil coccoid kerogen and background kerogen in the matrix.

Type of sample	Mean RIP	error (1 s.d.)	n
Coccoids, bedding plane	3.9	0.3	33
Coccoids, cross section	3.8	0.3	20
Coccoids, all	3.9	0.3	53
Matrix kerogen	3.7	0.4	10

SUPPLEMENTARY REFERENCES

Kamber, B.S., and Whitehouse, M.J., 2007, Micro-scale sulphur isotope evidence for sulphur cycling in the late Archean shallow ocean: Geobiology, v. 5, p. 5–17, doi:10.1111/j.1472-4669.2006.00091.x.

Kaufman, A.J., Johnston, D.T., Farquhar, J., Masterson, A.L., Lyons, T.W., Bates, S., Anbar, A.D., Arnold, G.L., Garvin, J., and Buick, R., 2007, Late Archean biospheric oxygenation and atmospheric evolution: Science, v. 317, p. 1900–1903, doi:10.1126/science.1138700.

Schopf, J.W., and Kudryavtsev, A.B., 2009, Confocal laser scanning microscopy and Raman imagery of ancient microscopic fossils: Precambrian Research, v. 173, no. 1-4, p. 39–49, doi: 10.1016/j.precamres.2009.02.007.

Schopf, J.W., Kudryavtsev, A.B., Agresti, D.G., Czaja, A.D., and Wdowiak, T.J., 2005, Raman imagery: a new approach to assess the geochemical maturity and biogenicity of permineralized Precambrian fossils: Astrobiology, v. 5, no. 3, p. 333–371.

Schopf, J.W., Sergeev, V.N., and Kudryavtsev, A.B., 2016, A new approach to ancient microorganisms: taxonomy, paleoecology, and biostratigraphy of the Lower Cambrian Berkuta and Chulaktau microbiotas of South Kazakhstan: J Paleontol, v. 89, no. 5, p. 695–729, doi: 10.1017/jpa.2015.56.

Schopf, J.W., Tripathi, A.B., and Kudryavtsev, A.B., 2006, Three-dimensional confocal optical imagery of Precambrian microscopic organisms: Astrobiology, v. 6, no. 1, p. 1–16.

Sumner, D.Y., 1997, Carbonate precipitation and oxygen stratification in late Archean seawater as deduced from facies and stratigraphy of the Gamohaan and Frisco formations, Transvaal Supergroup, South Africa: American Journal of Science, v. 297, no. 5, p. 455–487.